



Leptonic meson decays into invisible ALP

J. Alda Gallo^{a,b,c}, A.W.M. Guerrero^{c,*}, S. Peñaranda^{a,b}, S. Rigolin^c

^a *Departamento de Física Teórica, Facultad de Ciencias, Universidad de Zaragoza, Pedro Cerbuna 12, E-50009 Zaragoza, Spain*

^b *Centro de Astropartículas y Física de Altas Energías (CAPA), Universidad de Zaragoza, Zaragoza, Spain*

^c *Dipartimento di Fisica e Astronomia "G. Galilei", Università degli Studi di Padova e Istituto Nazionale Fisica Nucleare, Sezione di Padova, I-35131 Padova, Italy*

Received 22 February 2022; received in revised form 9 April 2022; accepted 12 April 2022

Available online 19 April 2022

Editor: Tommy Ohlsson

Abstract

The theoretical calculation of pseudo-scalar leptonic decay widths into an invisible ALP, $M \rightarrow \ell \nu_\ell a$, is reviewed. Assuming generic flavor-conserving ALP couplings to SM fermions and a generic ALP mass, m_a , the latest experimental results for pseudo-scalar leptonic decays are used to provide updated bounds on the ALP-fermion Lagrangian sector. Constrains on the ALP-quark couplings obtained from these channels are not yet competitive with the ones derived from FCNC processes, like $M \rightarrow Pa$ decays. These leptonic decays can, however, provide the most stringent model-independent upper bounds on ALP-leptons couplings for m_a in the (sub)–GeV range.

© 2022 The Author(s). Published by Elsevier B.V. This is an open access article under the CC BY license (<http://creativecommons.org/licenses/by/4.0/>). Funded by SCOAP³.

1. Introduction

Light pseudo-scalar particles naturally arise in many extensions Beyond the Standard Model (BSM) of particle physics, as they are a common feature of any model endowed with a global $U(1)_{PQ}$ symmetry spontaneously broken at a scale $f_a \gg v$. Small breaking terms of the global $U(1)_{PQ}$ symmetry are needed for providing a mass term, $m_a \ll f_a$, to the (pseudo) Nambu-Goldstone boson (pNGB). Sharing a common nature with the QCD axion [1–3], these classes of

* Corresponding author.

E-mail address: guerrera@pd.infn.it (A.W.M. Guerrero).

pNGBs are generically dubbed as Axion-Like Particles (ALPs). The key difference between the QCD axion and a generic ALP can be summarized in the fact that ALPs do not need to satisfy the well-known constraint [3], $m_a f_a \approx m_\pi f_\pi$, that bounds the QCD axion mass and the $U(1)_{PQ}$ symmetry breaking scale via QCD instanton effects. Therefore, in a generic ALP framework, one can assume the ALP mass being determined by some unspecified UV physics, and, consequently, m_a and f_a can be taken as independent parameters.

The ALP parameter space has been intensively explored in several terrestrial facilities, covering a wide energy range [4–13], as well as by many astrophysical and cosmological probes [14–18]. The synergy of these experimental searches allows to access several orders of magnitude in ALP masses and couplings, cf. e.g. Ref. [19] and references therein. While astrophysics and cosmology impose severe constraints on very light ALPs, the most efficient probes of weakly-coupled particles in the MeV-GeV range come from experiments acting on the precision frontier [20]. Fixed-target facilities such as E949 [21–23], NA62 [24,25] and KOTO [26] and the proposed SHiP [27] and DUNE [28] experiments can be very efficient to constrain long-lived particles. Furthermore, the rich ongoing research program in the B -physics experiments at LHCb [29,30] and the B -factories [31–39] offers several possibilities to probe ALP couplings in ALP mass regions not completely explored yet.

The main goal of this letter, is the detailed analysis of pseudo-scalar meson leptonic decays, $M \rightarrow \ell \nu_\ell a$, with an ALP escaping the detector or decaying into an “invisible” sector. These decay channels were previously analyzed in [40] for a massless ALP and for a universal ALP-fermion coupling. Here, a generic ALP mass and generic, yet flavor-conserving, ALP couplings are going to be considered. Therefore, independent limits to both quarks and leptons couplings to ALP are going to be derived. The bounds obtained for the couplings of ALPs to leptons are the most stringent to date. Finally, a factor 2 misprint in Eq. (15) of [40] (and equivalently a factor 4 misprint in the hadronic contribution of Eq. (17) of [40]) is going to be corrected.

2. Leptonic meson decays in ALP

The most general effective Lagrangian describing ALP interactions with SM fermions, including operators up to dimension five and assuming flavor conserving couplings reads:

$$\delta \mathcal{L}_{\text{eff}}^{a,MFV} = -\frac{\partial_\mu a}{2f_a} \sum_{i=fer} c_i \bar{\psi}_i \gamma^\mu \gamma_5 \psi_i = i \frac{a}{f_a} \sum_{i=fer} c_i m_i \bar{\psi}_i \gamma_5 \psi_i. \quad (1)$$

The Lagrangian in Eq. (1) depends only on nine independent flavor diagonal couplings, c_i , once fermionic vector-current conservation and massless neutrinos are implied. It might be useful, for simplifying intermediate calculations, and explicitly showing the mass dependence of ALP-fermion couplings, to write the effective Lagrangian in the “Yukawa” basis instead of the “derivative” one. The two versions of the effective Lagrangian in Eq. (1) are equivalent up to operators of $O(1/f_a^2)$.

Using the effective Lagrangian of Eq. (1) one can calculate the leptonic decay rates of pseudo-scalar mesons, $M \rightarrow \ell \nu_\ell a$, with the ALP sufficiently long-lived to escape the detector without decaying (or decaying into invisible channels). In such a case the only possible ALP signature is its missing energy/momentum. In the following, M_M and P_M will denote the mass and 4-momentum of the decaying meson, while leptons and ALP masses and 4-momenta will be indicated with m_ℓ , m_a , p_ℓ , p_ν and p_a respectively. Neutrinos will be assumed massless.

Charged pseudo-scalar meson decays proceed through the s -channel tree-level diagrams of Fig. 1, where only the diagrams where the ALP is emitted from the M -meson are shown. The di-

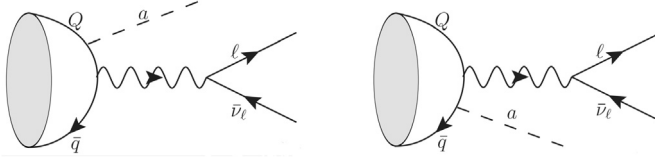


Fig. 1. Tree level contributions to the $M \rightarrow \ell \nu_\ell a$ amplitude, with the ALP emitted from the M meson. The diagram where the ALP is emitted from the charged lepton is straightforward.

agram where the ALP is emitted from the charged lepton follows straightforwardly, while the one with the ALP emitted from the W^+ internal line automatically vanishes, being the W^+W^- -ALP coupling proportional to the fully antisymmetric 4D tensor. In the following, the derivation of the decay amplitude for the channel in which the ALP is emitted from the initial quarks or from the final charged lepton are discussed separately, as they need two different hadronization treatments.

2.1. Hadronic ALP emission

The two diagrams depicted in Fig. 1 represent the contributions to the $M \rightarrow \ell \nu_\ell a$ decay in which the parent meson constituent quarks emit the ALP and then annihilate into a virtual W boson, producing the final leptons. One refers to this case as hadronic ALP emission. The corresponding amplitude¹ can be written as:

$$\mathcal{M}_h = \langle 0 | \bar{q} \Gamma_h^\mu Q | M \rangle (\bar{\ell} \gamma_\mu P_L \nu_\ell), \tag{2}$$

with Γ_h^μ given by

$$\Gamma_h^\mu = -\frac{4G_F}{\sqrt{2}} V_{qQ} \left(\frac{c_Q m_Q}{f_a} \gamma^\mu P_L \frac{\not{p}_a - \not{p}_Q + m_Q}{m_a^2 - 2p_a \cdot p_Q} \gamma_5 - \frac{c_q m_q}{f_a} \gamma_5 \frac{\not{p}_a - \not{p}_q - m_q}{m_a^2 - 2p_a \cdot p_q} \gamma^\mu P_L \right). \tag{3}$$

In Eq. (3) p_q and p_Q are the initial quarks momenta, with c_q and c_Q the corresponding ALP-fermion couplings.

The calculation of the $\langle 0 | \bar{q} \Gamma_h^\mu Q | M \rangle$ hadronic matrix element in Eq. (2) is complicated by the fact that the meson is a bound state of quarks and one must assume a model to describe the effective quark-antiquark momenta distribution. This can be done following the Lepage–Brodsky technique [41,42]. In the case of a massless ALP and universal ALP-fermion couplings this amplitude have been firstly derived in [40].

Following [40–42], the ground state of a meson M is parameterized with the wave–function

$$\Psi_M(x) = \frac{1}{4} \phi_M(x) \gamma^5 (\not{P}_M + g_M(x) M_M). \tag{4}$$

In Eq. (4), with x one typically denotes the fraction of the momentum carried by the heaviest quark in the meson. The function $\phi_M(x)$ describes the meson’s quark momenta distribution, that for heavy and light mesons reads, respectively:

$$\phi_H(x) \propto \left[\frac{\xi^2}{1-x} + \frac{1}{x} - 1 \right]^{-2}, \quad \phi_L(x) \propto x(1-x), \tag{5}$$

¹ For definiteness, the leptonic current is written assuming a negative charged meson $M = \bar{q}Q$ state, being q a light up-type quark and Q an heavy down-type one.

with the normalization fixed such that:

$$\int_0^1 dx \phi_M(x) = 1. \tag{6}$$

The parameter ξ in $\phi_H(x)$ is a small parameter typically of $O(m_q/m_Q)$, being q and Q the light and heavy quark in the meson. The mass function $g_M(x)$ is usually taken to be a constant varying from $g_H(x) \approx 1$ and $g_L(x) \ll 1$ for a heavy or a light meson. There are of course mesons that are neither heavy nor light, and a different parametrization is required, e.g. a Kaon or a D -meson. Let us study the two extreme cases with the K -meson considering either light (i.e. assuming an exact global $SU(3)$ symmetry) or as an heavy meson (i.e. $m_s \gg m_u, m_d$). In [13] it was argued that to consider these “in-between” states one should use the heavy mesons wave functions with the modified low-energy masses defined as $\hat{m}_q = m_q + \Lambda$ and $\hat{m}_Q = m_Q + \Lambda$, where $\Lambda = (M_M - m_q - m_Q)/2$ is a parameter of the order of the meson’s mass. It was also shown that this choice is a conservative one as using the light-meson wave function one has, at least in the massless ALP limit, an enhancement of a factor $3/2$.

The hadronic matrix element can then be obtained by integrating, over the momentum fraction x , the trace of the Γ_h^μ amplitude multiplied by the meson wave-function $\Psi_M(x)$:

$$\langle 0 | \bar{q} \Gamma_h^\mu Q | M \rangle \equiv i f_M \int_0^1 dx \text{Tr} [\Gamma_h^\mu \Psi_M(x)], \tag{7}$$

with the meson decay constants f_M defined as:

$$\langle 0 | \bar{q} \gamma^\mu \gamma_5 Q | M \rangle = i f_M P_M^\mu. \tag{8}$$

In Eqs. (4)–(7), a slightly different notation with respect to the referred literature is used. In particular the functions $\phi_M(x)$ have been normalized to one, in such a way that in Eq. (7) the mesonic form factor can be explicitly factorized.

Inserting Eq. (3) and Eq. (4) into Eq. (7), and defining the initial quark momenta as:

$$p_q = (1 - x) P_M, \quad p_Q = x P_M$$

one obtains the following decay amplitudes for the meson ALP-emission process:

$$\mathcal{M}_h = \frac{4i G_F V_{qQ} f_M}{\sqrt{2} f_a 2 p_a \cdot P_M} \frac{M_M^2}{M_M} \left[c_Q \frac{m_Q}{M_M} \Phi_M^{(Q)}(m_a^2) - c_q \frac{m_q}{M_M} \Phi_M^{(q)}(m_a^2) \right] (\bar{\ell} \not{p}_a P_L v_\ell) \tag{9}$$

where the functions $\Phi_M^{(q,Q)}(m_a^2)$ contain the integrals over the quark momentum fraction and are defined respectively as:

$$\Phi_M^{(q)}(m_a^2) = \int_0^{1-\delta_M} \frac{p_a \cdot P_M}{m_a^2 - 2(1-x) p_a \cdot P_M} \phi_M(x) g_M(x) dx$$

$$\Phi_M^{(Q)}(m_a^2) = \int_{\delta_M}^1 \frac{p_a \cdot P_M}{m_a^2 - 2x p_a \cdot P_M} \phi_M(x) g_M(x) dx.$$

The presence of the kinematical cutoff $\delta_M = m_a/(2M_M)$ prevents the appearance of unphysical bare singularities.

One can check the calculation done in Ref. [40] by taking the $m_a = 0$ limit in Eq. (9) and by setting $c_q = c_Q = 2$, as demanded by the different normalization of the corresponding ALP-fermion couplings introduced in the effective Lagrangians. Notice that

$$\left[\frac{m_b}{M_B} \Phi_B^{(b)}(0) - \frac{m_u}{M_B} \Phi_B^{(u)}(0) \right] = 2\sqrt{6} \Phi(m_b, M_B) \quad (10)$$

with $\Phi(m_b, M_B)$ the integral defined in Ref. [40]. Doing all these replacements one realizes that Eq. (15) of Ref. [40] is wrong and 1/2 of the result obtained from Eq. (9).

2.2. Leptonic ALP emission

The leptonic decay amplitude for the lepton ALP-emission process can be easily obtained by using the definition of the meson form factors of Eq. (8), giving

$$\mathcal{M}_\ell = \langle 0 | \bar{q} \gamma_\mu P_L Q | M \rangle (\bar{\ell} \Gamma_\ell^\mu \nu_\ell),$$

with

$$\Gamma_\ell^\mu = -\frac{4G_F}{\sqrt{2}} V_{qQ} \left(\frac{c_\ell m_\ell}{f_a} \gamma_5 \frac{\not{p}_a + \not{p}_\ell + m_\ell}{m_a^2 + 2p_a \cdot p_\ell} \gamma^\mu P_L \right). \quad (11)$$

In Eq. (11) p_ℓ dubs the momentum of the final charged lepton. By making use of all the Dirac matrices relations one obtains:

$$\mathcal{M}_\ell = -\frac{4iG_F}{\sqrt{2}} V_{qQ} \frac{f_M}{f_a} \left[c_\ell m_\ell (\bar{\ell} P_L \nu_\ell) - \frac{c_\ell m_\ell^2}{m_a^2 + 2p_a \cdot p_\ell} (\bar{\ell} \not{p}_a P_L \nu_\ell) \right]. \quad (12)$$

From Eq. (12), by setting $m_a = 0$ and $c_\ell = 2$ one recovers correctly the result in Eq. (7) of Ref. [40].

2.3. Differential decay rate

For the 3-body decay at hand, and assuming a massless neutrino, one can define the following Mandelstam variables:

$$s = (P_M - p_\ell)^2 = (p_\nu + p_a)^2 = M_M^2 + m_\ell^2 - 2M_M \omega_\ell \quad (13)$$

$$t = (P_M - p_\nu)^2 = (p_\ell + p_a)^2 = M_M^2 - 2M_M \omega_\nu \quad (14)$$

$$u = (P_M - p_a)^2 = (p_\ell + p_\nu)^2 = M_M^2 + m_a^2 - 2M_M \omega_a \quad (15)$$

with the energy conservation providing the identity:

$$s + t + u = M_M^2 + m_\ell^2 + m_a^2.$$

The differential 3-body decay rate of any scalar particle in its rest frame can be simply written as function of two independent final energies ω_i , or equivalently of the two independent Mandelstam variables, as

$$(d\Gamma_M)_{RF} = \frac{1}{(2\pi)^3} \frac{1}{8M_M} |\overline{\mathcal{M}}_M|^2 d\omega_\ell d\omega_a = \frac{1}{(2\pi)^3} \frac{1}{32M_M^3} |\overline{\mathcal{M}}_M|^2 ds du \quad (16)$$

with $\mathcal{M}_M = \mathcal{M}_\ell + \mathcal{M}_h$. The Feynman amplitude squared reads:

$$|\overline{\mathcal{M}_\ell}|^2 = C_M c_\ell^2 \frac{m_\ell^2}{M_M^2} \left\{ \frac{p_\ell \cdot p_\nu}{M_M^2} - \frac{m_\ell^2}{M_M^2} \left(\frac{p_a \cdot p_\nu}{m_a^2 + 2 p_a \cdot p_\ell} + m_a^2 \frac{p_\nu \cdot (p_a + p_\ell)}{(m_a^2 + 2 p_a \cdot p_\ell)^2} \right) \right\} \quad (17)$$

$$|\overline{\mathcal{M}_h}|^2 = C_M \left[c_Q \frac{m_Q}{M_M} \Phi_M^{(Q)}(m_a^2) - c_q \frac{m_q}{M_M} \Phi_M^{(q)}(m_a^2) \right]^2 \frac{2(p_a \cdot p_\ell)(p_a \cdot p_\nu) - m_a^2 p_\ell \cdot p_\nu}{(p_a \cdot P_M)^2} \quad (18)$$

$$\overline{\mathcal{M}_h \mathcal{M}_\ell^*} = C_M c_\ell \frac{m_\ell^2}{M_M^2} \left[c_Q \frac{m_Q}{M_M} \Phi_M^{(Q)}(m_a^2) - c_q \frac{m_q}{M_M} \Phi_M^{(q)}(m_a^2) \right] \frac{m_a^2 (p_a \cdot p_\nu + p_\ell \cdot p_\nu)}{(m_a^2 + 2 p_a \cdot p_\ell)(p_a \cdot P_M)} \quad (19)$$

with the overall constant factor defined as:

$$C_M = 4 G_F^2 |V_{qQ}|^2 M_M^4 \frac{f_M^2}{f_a^2}.$$

One can notice from Eq. (19), that the mixed product is proportional both to the ALP and the charged lepton masses and, consequently, can be neglected either for a massless ALP or for meson decays to a light charged lepton.

The total decay rate, for a general ALP mass, can be obtained by numerically integrating the differential decay rate of Eq. (16) in the kinematically allowed region. On the other hand, the massless ALP limit can be easily integrated analytically. By setting $m_a = 0$ one obtains:

$$\Gamma_{M \rightarrow \ell \nu_\ell a} = \frac{G_F^2 |V_{qQ}|^2 M_M^5 f_M^2}{384 \pi^2 f_a^2} \left\{ c_\ell^2 \left(2\rho^2 + 3\rho^4 + 12\rho^4 \log \rho - 6\rho^6 + \rho^8 \right) + \left[\frac{c_Q m_Q}{M_M} \Phi_M^{(Q)}(0) - \frac{c_q m_q}{M_M} \Phi_M^{(q)}(0) \right]^2 \left(1 - 6\rho^2 - 12\rho^4 \log \rho + 3\rho^4 + 2\rho^6 \right) \right\}. \quad (20)$$

For $c_\ell = c_q = c_Q = 2$ one recovers an agreement with the leptonic part of the decay rate in Eq. (17) of Ref. [40], while the hadronic part is wrong and 1/4 of the result in Eq. (20), consistently with what obtained from the Feynman amplitude check.

3. Bounds on ALP-fermion couplings

Pseudo-scalar leptonic decay experiments can be used to constraint flavor-diagonal ALP-fermion couplings of Eq. (1) via the ALP (invisible) decay rate derived in the previous section. Leptonic B -decays have been measured at B -factories, latest BELLE data for electron, muon and tau channel can be found in [43–45], respectively. Charmed meson decays have been measured at BESS (see [46–48] for D and [49,50] for D_s decays respectively) and at BELLE [51]. Leptonic Kaon decays have been measured by KLOE and NA62 [52–54]. In Table 1 available experimental determinations for the leptonic pseudo-scalar decay branching ratios are summarized and the lowest order SM predictions are shown for comparison.

The main assumption underlying the following phenomenological analysis is that the ALP lifetime is sufficiently long to escape the detector (i.e. $\tau_a \gtrsim 100$ ps) or alternatively that the ALP is mainly decaying into a, not better specified, invisible sector. In both cases, the ALP signature is a missing energy/momentum, just as for neutrinos. In this scenario, the simplest

Table 1

Lowest order SM predictions and experimental constraints on the considered $M \rightarrow \ell \nu$ decay branching ratios.

Channel	SM branching ratio	Experiment	Ref.
$B^\pm \rightarrow e^\pm \bar{\nu}_e$	8.37×10^{-12}	$< 9.8 \times 10^{-7}$	[43]
$B^\pm \rightarrow \mu^\pm \bar{\nu}_\mu$	3.57×10^{-7}	$(5.3 \pm 2 \pm 0.9) \times 10^{-7}$	[44]
$B^\pm \rightarrow \tau^\pm \bar{\nu}_\tau$	7.95×10^{-5}	$(7.2 \pm 2.7 \pm 1.1) \times 10^{-5}$	[45]
$D^\pm \rightarrow e^\pm \bar{\nu}_e$	9.51×10^{-9}	$< 8.8 \times 10^{-6}$	[46]
$D^\pm \rightarrow \mu^\pm \bar{\nu}_\mu$	4.04×10^{-4}	$(3.71 \pm 0.19 \pm 0.06) \times 10^{-4}$	[47]
$D^\pm \rightarrow \tau^\pm \bar{\nu}_\tau$	1.08×10^{-3}	$(1.2 \pm 0.24 \pm 0.12) \times 10^{-3}$	[50]
$D_s^\pm \rightarrow e^\pm \bar{\nu}_e$	1.24×10^{-7}	$< 8.3 \times 10^{-5}$	[51]
$D_s^\pm \rightarrow \mu^\pm \bar{\nu}_\mu$	5.28×10^{-3}	$(5.49 \pm 0.17) \times 10^{-3}$	[48]
$D_s^\pm \rightarrow \tau^\pm \bar{\nu}_\tau$	5.15×10^{-2}	$(4.83 \pm 0.65 \pm 0.26) \times 10^{-2}$	[49]
$K^\pm \rightarrow e^\pm \bar{\nu}_e$	1.62×10^{-5}	$(1.582 \pm 0.007) \times 10^{-5}$	[54]
$K^\pm \rightarrow \mu^\pm \bar{\nu}_\mu$	0.629	0.6356 ± 0.0011	[54]

Table 2

Limits on the $U(1)_{PQ}$ scale f_a derived from leptonic pseudo-scalar meson decays, setting the relevant ALP-fermion coupling equal to one, with all the other couplings vanishing.

Channel	f_a [GeV] up-quark		f_a [GeV] down-quark		f_a [GeV] lepton	
	$m_a = 0$	$m_a = M_M/2$	$m_a = 0$	$m_a = M_M/2$	$m_a = 0$	$m_a = M_M/2$
$B^\pm \rightarrow e^\pm \bar{\nu}_e$	2.8	0.079	4	1.3	0.0005	0.00013
$B^\pm \rightarrow \mu^\pm \bar{\nu}_\mu$	6	0.16	8.3	2.7	0.2	0.06
$B^\pm \rightarrow \tau^\pm \bar{\nu}_\tau$	0.38	0.006	0.5	0.065	0.2	0.05
$D^\pm \rightarrow e^\pm \bar{\nu}_e$	6	2.1	5.7	0.86	0.02	0.00053
$D^\pm \rightarrow \mu^\pm \bar{\nu}_\mu$	4	1.3	3.7	0.56	0.27	0.070
$D^\pm \rightarrow \tau^\pm \bar{\nu}_\tau$	0.007		0.007		0.006	
$D_s^\pm \rightarrow e^\pm \bar{\nu}_e$	8	3	8.2	1.9	0.002	0.00066
$D_s^\pm \rightarrow \mu^\pm \bar{\nu}_\mu$	5.5	2	5.7	1.3	0.3	0.09
$D_s^\pm \rightarrow \tau^\pm \bar{\nu}_\tau$	0.02		0.01		0.02	
$K^\pm \rightarrow e^\pm \bar{\nu}_e$	249.	87	170	10	0.243	0.06
$K^\pm \rightarrow \mu^\pm \bar{\nu}_\mu$	1.7	0.5	1.2	0.05	0.32	0.06

way to constrain ALP-fermion couplings is then to saturate the $1-\sigma$ experimental limits on the corresponding leptonic branching ratio adding the leptonic ALP decay to the leptonic SM amplitude. No kinematical constraint (2-body vs 3-body decay) is used in the analysis at this stage.

The derived bounds on the $U(1)_{PQ}$ breaking scale f_a are shown in Table 2. These values have been obtained by setting the relevant ALP-fermion coupling to one, with all the others vanishing. The results are provided for two reference values of the ALP mass $m_a = 0$ GeV and $m_a = M_M/2$ GeV, showing the variability range that should be expected for a massive vs (almost) massless ALP. As an example, the first row in Table 2 should be read as follows: the ‘‘up-quark’’ columns represent the f_a limits obtained by setting $c_u = 1$ and $c_b = c_e = 0$ for the two reference values of m_a , the ‘‘down-quark’’ columns represent the limits obtained by setting $c_b = 1$ and $c_u = c_e = 0$, and finally the values in the ‘‘lepton’’ columns are obtained by setting $c_e = 1$ and $c_u = c_b = 0$.

For heavy pseudo-scalar mesons, such as B , D and D_s , the formulas described in Sec. 2 are straightforward. These mesons are very well described by the heavy wave function $\phi_H(x)$

in Eq. (5), with $g_M = 1$. Constituent quark masses should be used for partons, instead of bare masses, i.e. $M_M = \hat{m}_Q + \hat{m}_q$ (being $\hat{m}_Q \approx m_Q$) with Q and q the heavy and light quark in the meson, respectively. The Kaon sector is more delicate as Kaons cannot be treated fully consistently neither as heavy or as light mesons [55]. Therefore, as the Kaon mass is not too far from Λ_{QCD} , the Brodsky–Lepage method introduces larger hadronic uncertainties compared to the heavy mesons case. Here, conservatively, the heavy meson wave–function is used,² with $g_K = 1$ and the partonic masses defined as $\hat{m}_u = m_u + \Lambda$ and $\hat{m}_s = m_s + \Lambda$ with $\Lambda = (M_K - m_u - m_s)/2$ a parameter of order Λ_{QCD} . Different choices for g_K , lead to different limits on f_a that can be obtained by a simple rescaling of the ones shown in the last two rows of Table 2, i.e. $f'_a = g_K f_a$. Therefore, smaller values for g_K result in less stringent bounds for the $U(1)_{PQ}$ scale.

One can immediately realize that the f_a bounds shown in Table 2 from up-type and down-type ALP-quark sectors are far from being competitive with the ones derived from FCNC processes, like $K \rightarrow \pi a$ or $B \rightarrow Ka$. For example, from [38], one can infer a limit $f_a \gtrsim 10^9$ MeV stemming from the top-enhanced penguin contribution, assuming $c_t = 1$. Tree–level diagram contributions to FCNC processes can provide constraints on lighter quark sectors [13], giving limits on f_a in the range $f_a \gtrsim 10^6 - 10^7$ MeV. From $Y(ns)$ decays one can obtain a constraint of the same order for the bottom sector [39]. The only pseudo–scalar meson leptonic channel that provide almost comparable bounds on the quark sector is the $K^\pm \rightarrow e^\pm \bar{\nu}_e$ decay, while most the other pseudo–scalar leptonic decays provide limits in the ballpark $f_a \gtrsim 10^3 - 10^4$ MeV for the light lepton decays and $f_a \gtrsim 10^1 - 10^2$ MeV for the τ ones.

Nonetheless, pseudo–scalar meson leptonic decays can be still very useful, as they provide the best present limits on the ALP–lepton sector for an ALP with m_a in the (sub)–GeV range, bounding $f_a \gtrsim 10^2 - 10^3$ MeV for most of the available channels. Typically, the muon sector gives better limits on f_a as it combines experimental data with relatively smaller errors and a not too large lepton mass suppression of the amplitude in Eq. (17). The electron sector suffers from a larger mass suppression and typically provides bounds on $f_a \gtrsim 10^5 - 10^6$ MeV, with the only exception of the $K^\pm \rightarrow e^\pm \bar{\nu}_e$ channel benefiting from its highly precise determination.³ Furthermore, in this ALP mass range, the results presented here on the electron coupling c_e can be complementary with present and future ALP-DM searches like EDELWEISS [56] and LDMX [57] and reactor searches at CONNIE, CONUS, MINE, and ν -cleus [58].

The same information can be visually obtained from the plots in Fig. 2 and Fig. 3, where the dependence of the c_i/f_a bounds on the ALP mass is shown for the ALP couplings to up-type and down-type quarks (Fig. 2 (a) and Fig. 2 (b) respectively) and for the ALP couplings to charged leptons (Fig. 3 (a)). As previously noticed, the $K^\pm \rightarrow e^\pm \bar{\nu}_e$ channel is the most promising one, putting bounds on $c_{u,s}/f_a \lesssim 5 \text{ TeV}^{-1}$, while most of the other channels are providing limits $c_{u,c,s,b}/f_a \lesssim 10^2 - 10^3 \text{ TeV}^{-1}$, still far from the perturbativity region for $f_a = 1 \text{ TeV}$. Concerning the ALP-charged lepton coupling notice that the best limits come from μ decay channels, bounding $c_\mu/f_a \lesssim 10^3 - 10^4 \text{ TeV}^{-1}$. Measures of c_τ are still limited by worse experimental resolution providing bounds $c_\tau/f_a \lesssim 10^5 \text{ TeV}^{-1}$. Sensitivity to the ALP-electron coupling c_e is obviously suppressed by the tiny electron mass giving $c_e/f_a \lesssim 10^6 - 10^7 \text{ TeV}^{-1}$.

The results presented here represent an improvement of at least one order of magnitude compared with limits obtained in Tab. III of [40]. Three main reasons can be advocated: i) first of all,

² Using the heavy meson wave–function $\phi_H(x)$ one obtains a decay amplitude roughly 2/3 of one obtained using the light meson wave–function, $\phi_L(x)$. A detailed analysis of the hadronic uncertainties for K decays can be found in [13].

³ Recall, however, that caution should be used when handling K data as a larger hadronic uncertainty has to be accounted for, unavoidably.

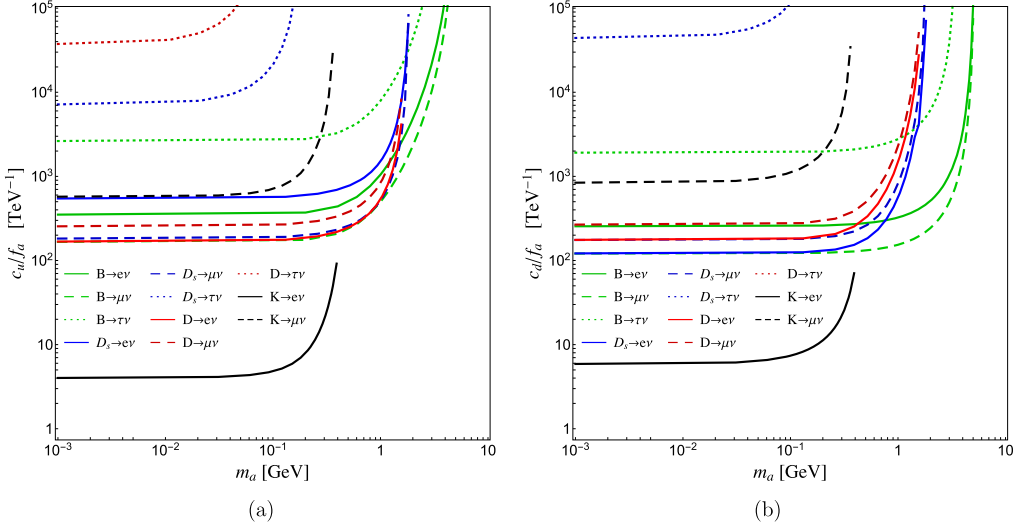


Fig. 2. Limits on the coupling (a) c_u/f_a and (b) c_d/f_a derived from the leptonic meson decay indicated in the legend, as function of the ALP mass m_a .

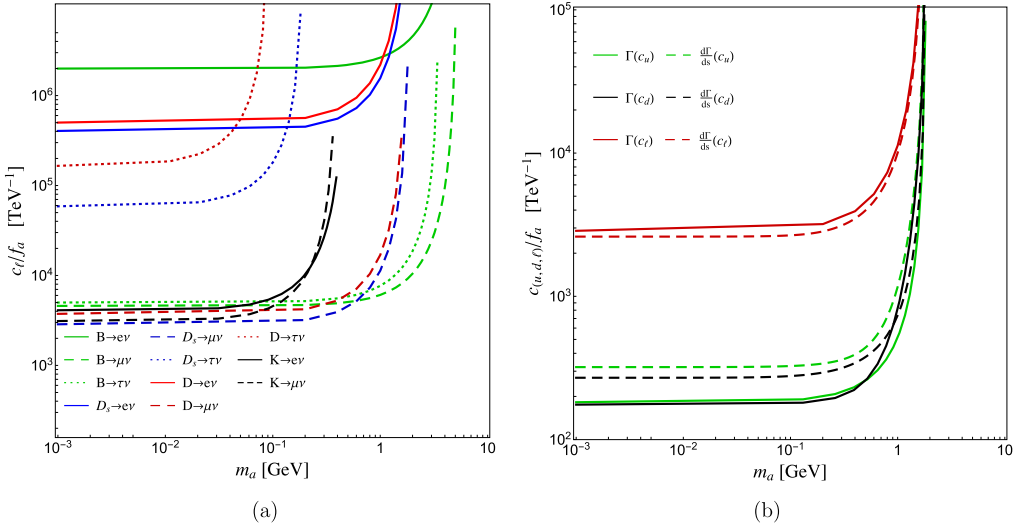


Fig. 3. Limits on the coupling c_l/f_a (a) derived from the leptonic meson decays indicated in the legend, as function of the ALP mass m_a . Figure (b) shows the limits obtained on all the couplings from the analysis of the $D_s \rightarrow \mu \nu_\mu a$ decay using the experimental BR (full lined) and the missing mass distribution (dashed line).

since the publishing of [40], experimental determination of pseudo-scalar leptonic decays has typically improved by roughly a factor ten, leading to more stringent bounds on f_a , ii) moreover, one has to recall that the leading hadronic contribution in Eq. (17) of [40] underestimates by 1/4 the ALP branching ratio, resulting again in lower f_a bounds, iii) finally, assuming a universal ALP-fermion coupling results in a parametric cancellation, clearly shown in Eq. (9) and Eq. (10) once $c_q = c_Q$ is assumed, causing a lost in sensitivity that numerically can be estimated in the

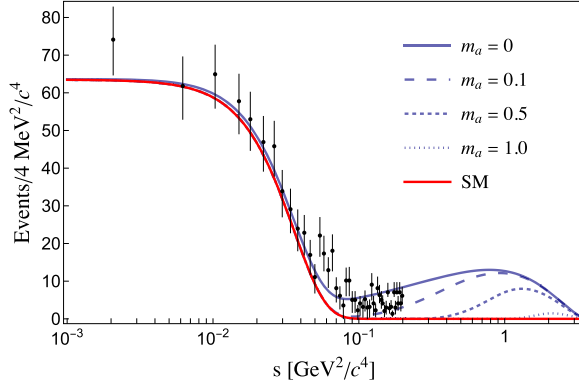


Fig. 4. Missing mass squared distribution for the $D_s \rightarrow \mu \nu \mu$ decay from BESSIII collaboration [48]. The red solid line corresponds to the SM smeared two-body differential decay rate $d\Gamma/ds$. Blue curves represent the predicted distributions once the three-body $D_s \rightarrow \mu \nu \mu a$ decay is included, plotted for different values of the ALP mass, m_a in GeV.

50%–70% range.⁴ One might consider more than one parameter at once when projecting the bounds, of course as discussed above a parametric flat direction would arise, at least in the ALP massless limit. This cancellation effect quickly fades away as the ALP mass increases, as it can be deduced from the $m_a = 0$ and $m_a = M_M/2$ columns of Table 2.

All the bounds shown up to now have been extracted using exclusively information inferred from the total decay rate. One may think that stronger constraints should be derived from the differential decay rate $d\Gamma/d\omega_\ell$ (or equivalently $d\Gamma/ds$) obtained integrating Eq. (16) over the ALP energy ω_a (or over the Mandelstam variable u), thus exploiting the different leptonic energy distribution characterizing two-body vs three-body decays. The SM two-body decay distribution is peaked around vanishing missing mass $s = m_\nu^2 \approx 0$, and therefore any excess of events with $s > 0$ could be an indication of a three-body decay, once SM backgrounds (like $D_s \rightarrow \mu \nu \mu \gamma$ with ω_γ below the detection energy threshold) have been opportunely accounted for. As an example, in Fig. 3(b), the comparison between the limits on the c_i/f_a coefficients obtained from the differential decay rate analysis for the $D_s \rightarrow \mu \nu \mu$ decay observed by BESIII [48] (dashed lines) and the bounds from the branching ratio (solid lines) are shown. The two methods give comparable bounds, with limits obtained from the differential decay rate analysis being somehow less stringent, showing that no clear improvement is obtained, with present data, by adding the available spectral information.

The reason can be easily understood by looking at Fig. 4. The red continuous line represents the experimentally smeared SM two body decays rate, $d\Gamma_{SM}/ds$, here shown only for $s > 0$, as shown in Fig. 2 of [48]. The $d\Gamma_{SM+NP}/ds$ distributions obtained including the three body decay $D_s \rightarrow \mu \nu \mu a$ for $c_i/f_a = 200 \text{ TeV}^{-1}$ and different values of the ALP mass, m_a are shown as blue curves. BESSIII collaboration provides data (dots with error bands) on the missing mass distribution only for $s < 0.2 \text{ GeV}^2/c^4$, while most of the NP signal lies above $s > 0.5 \text{ GeV}^2/c^4$. Consequently, less stringent limits on c_i/f_a can be obtained by using available spectral information. Same conclusions can be extrapolated from the other few analyses with public missing mass squared distributions. An improvement to the bounds on the ALP-fermion couplings ob-

⁴ A detailed and more qualitative discussion of this effect can be found in [13].

tained from the total decay rate would require to have access to the complete experimental data of signal and background distributions, and is beyond the reach of this letter.

4. Conclusions

A detailed analysis of the pseudo–scalar meson leptonic ALP decays, $M \rightarrow \ell \nu_\ell a$ has been presented. These decay channels were previously analyzed in Ref. [40] but only for a massless ALP and for a universal ALP–fermion coupling. Here we have considered a generic ALP mass along with a generic flavor structure for the couplings of the Axion–like particle to quarks and leptons. Moreover, a factor 2 misprint in Eq. (15) of Ref. [40] (and equivalently a factor 4 misprint in the hadronic contribution of Eq. (17) of Ref. [40]) has been addressed. Bounds on flavor diagonal ALP–fermion couplings are derived from the latest experimental limits on the corresponding leptonic decays. The stringent bounds on ALP–quarks couplings can be derived from the $K \rightarrow e \bar{\nu}_e a$ decay, with $c_{s,u}/f_a$ around 5 TeV^{-1} , barring large hadronic uncertainties. This bound is, however, still quite far from being competitive with the ones derived from the $K \rightarrow \pi a$ process (see for example [13] for a recent analysis). From heavier pseudo–scalar meson decay channels with a final electron or muon, one can derive bounds on ALP–quarks couplings, $c_q/f_a \gtrsim 10^2 \text{ TeV}^{-1}$. Typically, less stringent bounds can be obtained from the tau channels, mainly due to larger experimental uncertainties.

Nevertheless, pseudo–scalars leptonic decays can provide the most stringent independent upper bounds on ALP–leptons couplings, for and ALP mass, m_a , in the (sub)–GeV range. From D_s and B muon and tau decays one derives limits on $c_{\mu,\tau}/f_a$ around $5 \times 10^3 \text{ TeV}^{-1}$, in all the kinematically allowed m_a range. The most stringent limit on the ALP–electron coupling can be derived from the $K \rightarrow e \nu_e a$ decay, $c_e/f_a \lesssim 4 \times 10^3 \text{ TeV}^{-1}$, for $m_a \lesssim 0.3 \text{ GeV}$. For heavier ALP, D_s and B pseudo–scalar meson decays provide much softer bounds with $c_e/f_a \lesssim 10^6 \text{ TeV}^{-1}$. In the analysis of Ref. [40], these constraints were not available being their limits essentially referred to the dominant quark contributions. Present bounds on ALP–electron couplings can be complementary to those obtained from ALP–DM searches [59].

CRedit authorship contribution statement

All the authors have contributed equally to the scientific production, editing process, data analysis and presentation of this manuscript.

Declaration of competing interest

The authors declare that they have no known competing financial interests or personal relationships that could have appeared to influence the work reported in this paper.

Acknowledgements

The authors thank Javier Redondo, Maurizio Giannotti and Luca di Luzio for helpful comments and discussions. A.G. and S.R. acknowledge support from the European Union’s Horizon 2020 research and innovation programme under the Marie Skłodowska-Curie grant agreements 690575 (RISE InvisiblesPlus) and 674896 (ITN ELUSIVES). This project has received funding/support from the European Union’s Horizon 2020 research and innovation programme under the Marie Skłodowska-Curie grant agreement No. 860881-HIDDEN. The work of J. A. and S. P.

is partially supported by Spanish grants MINECO/FEDER grant FPA2015-65745-P, PGC2018-095328-B-I00 (FEDER/Agencia estatal de investigación) and DGIID-DGA No. 2015-E24/2. J. A. is also supported by the Departamento de Innovación, Investigación y Universidad of Aragón government, Grant No. DIIU-DGA and the Programa Ibercaja-CAI de Estancias de Investigación, Grant No. CB 5/21. J. A. thanks the warm hospitality of the Università degli Studi di Padova and Istituto Nazionale di Fisica Nucleare.

References

- [1] R.D. Peccei, Helen R. Quinn, CP conservation in the presence of instantons, *Phys. Rev. Lett.* 38 (1977) 1440–1443.
- [2] F. Wilczek, Problem of strong p and t invariance in the presence of instantons, *Phys. Rev. Lett.* 40 (Jan 1978) 279–282.
- [3] Steven Weinberg, A new light boson?, *Phys. Rev. Lett.* 40 (Jan 1978) 223–226.
- [4] Ken Mimasu, Verónica Sanz, ALPs at colliders, *J. High Energy Phys.* 06 (2015) 173, arXiv:1409.4792 [hep-ph].
- [5] Joerg Jaeckel, Michael Spannowsky, Probing MeV to 90 GeV axion-like particles with LEP and LHC, *Phys. Lett. B* 753 (2016) 482–487, arXiv:1509.00476 [hep-ph].
- [6] Martin Bauer, Matthias Neubert, Andrea Thamm, Collider probes of axion-like particles, *J. High Energy Phys.* 12 (2017) 044, arXiv:1708.00443 [hep-ph].
- [7] I. Brivio, M.B. Gavela, L. Merlo, K. Mimasu, J.M. No, R. del Rey, V. Sanz, ALPs effective field theory and collider signatures, *Eur. Phys. J. C* 77 (8) (2017) 572, arXiv:1701.05379 [hep-ph].
- [8] G. Alonso-Álvarez, M.B. Gavela, P. Quilez, Axion couplings to electroweak gauge bosons, *Eur. Phys. J. C* 79 (3) (2019) 223, arXiv:1811.05466 [hep-ph].
- [9] Cristian Baldenegro, Sylvain Fichet, Gero von Gersdorff, Christophe Royon, Searching for axion-like particles with proton tagging at the LHC, *J. High Energy Phys.* 06 (2018) 131, arXiv:1803.10835 [hep-ph].
- [10] Lucian Harland-Lang, Joerg Jaeckel, Michael Spannowsky, A fresh look at ALP searches in fixed target experiments, *Phys. Lett. B* 793 (2019) 281–289, arXiv:1902.04878 [hep-ph].
- [11] Jorge Martin Camalich, Maxim Pospelov, Pham Ngoc Hoa Vuong, Robert Ziegler, Jure Zupan, Quark flavor phenomenology of the QCD axion, *Phys. Rev. D* 102 (1) (2020) 015023, arXiv:2002.04623 [hep-ph].
- [12] Luca Di Luzio, Ramona Gröber, Paride Paradisi, Hunting for the CP violating ALP, arXiv:2010.13760 [hep-ph], Oct 2020.
- [13] Alfredo Walter, Mario Guerrero, Stefano Rigolin, Revisiting $K \rightarrow \pi a$ decays, *Eur. Phys. J. C* 82 (3) (2022) 192, arXiv:2106.05910 [hep-ph].
- [14] Davide Cadamuro, Javier Redondo, Cosmological bounds on pseudo Nambu-Goldstone bosons, *J. Cosmol. Astropart. Phys.* 02 (2012) 032, arXiv:1110.2895 [hep-ph].
- [15] Marius Millea, Lloyd Knox, Brian Fields, New bounds for axions and axion-like particles with keV-GeV masses, *Phys. Rev. D* 92 (2) (2015) 023010, arXiv:1501.04097 [astro-ph.CO].
- [16] Luca Di Luzio, Federico Mescia, Enrico Nardi, Redefining the axion window, *Phys. Rev. Lett.* 118 (3) (2017) 031801, arXiv:1610.07593 [hep-ph].
- [17] Prateek Agrawal, et al., Feebly-interacting particles: FIPs 2020 workshop report, arXiv:2102.12143 [hep-ph], Feb 2021.
- [18] Giuseppe Lucente, Pierluca Carenza, Supernova bound on axion-like particles coupled with electrons, arXiv:2107.12393 [hep-ph], Jul 2021.
- [19] Igor G. Irastorza, Javier Redondo, New experimental approaches in the search for axion-like particles, *Prog. Part. Nucl. Phys.* 102 (2018) 89–159, arXiv:1801.08127 [hep-ph].
- [20] Rouven Essig, et al., Working group report: new light weakly coupled particles, in: Community Summer Study 2013: Snowmass on the Mississippi, Oct 2013, arXiv:1311.0029 [hep-ph].
- [21] A.V. Artamonov, et al., Study of the decay $K^+ \rightarrow \pi^+ \nu \bar{\nu}$ in the momentum region $140 < P_{\pi^+} < 199$ MeV/c, *Phys. Rev. D* 79 (2009) 092004, arXiv:0903.0030 [hep-ex].
- [22] A.V. Artamonov, et al., New measurement of the $K^+ \rightarrow \pi^+ \nu \bar{\nu}$ branching ratio, *Phys. Rev. Lett.* 101 (2008) 191802, arXiv:0808.2459 [hep-ex].
- [23] S. Adler, et al., Measurement of the $K^+ \rightarrow \pi^+ \nu \bar{\nu}$ branching ratio, *Phys. Rev. D* 77 (2008) 052003, arXiv:0709.1000 [hep-ex].
- [24] Eduardo Cortina Gil, et al., Search for a feebly interacting particle X in the decay $K^+ \rightarrow \pi^+ X$, *J. High Energy Phys.* 03 (2021) 058, arXiv:2011.11329 [hep-ex].
- [25] Eduardo Cortina Gil, et al., Measurement of the very rare $K^+ \rightarrow \pi^+ \nu \bar{\nu}$ decay, arXiv:2103.15389 [hep-ex].

- [26] J.K. Ahn, et al., Search for the $K_L \rightarrow \pi^0 \nu \bar{\nu}$ and $K_L \rightarrow \pi^0 X^0$ decays at the J-PARC KOTO experiment, *Phys. Rev. Lett.* 122 (2) (2019) 021802, arXiv:1810.09655 [hep-ex].
- [27] Sergey Alekhin, et al., A facility to search for hidden particles at the CERN SPS: the SHiP physics case, *Rep. Prog. Phys.* 79 (12) (2016) 124201, arXiv:1504.04855 [hep-ph].
- [28] Kevin J. Kelly, Soubhik Kumar, Zhen Liu, Heavy axion opportunities at the DUNE near detector, *Phys. Rev. D* 103 (9) (2021) 095002, arXiv:2011.05995 [hep-ph].
- [29] Roel Aaij, et al., Search for hidden-sector bosons in $B^0 \rightarrow K^{*0} \mu^+ \mu^-$ decays, *Phys. Rev. Lett.* 115 (16) (2015) 161802, arXiv:1508.04094 [hep-ex].
- [30] R. Aaij, et al., Search for long-lived scalar particles in $B^+ \rightarrow K^+ \chi (\mu^+ \mu^-)$ decays, *Phys. Rev. D* 95 (7) (2017) 071101, arXiv:1612.07818 [hep-ex].
- [31] Eduard Masso, Ramon Toldra, On a light spinless particle coupled to photons, *Phys. Rev. D* 52 (1995) 1755–1763, arXiv:hep-ph/9503293.
- [32] A.J. Bevan, et al., The physics of the B factories, *Eur. Phys. J. C* 74 (2014) 3026, arXiv:1406.6311 [hep-ex].
- [33] Eder Izaguirre, Tongyan Lin, Brian Shuve, Searching for axion-like particles in flavor-changing neutral current processes, *Phys. Rev. Lett.* 118 (11) (2017) 111802, arXiv:1611.09355 [hep-ph].
- [34] Matthew J. Dolan, Torben Ferber, Christopher Hearty, Felix Kahlhoefer, Kai Schmidt-Hoberg, Revised constraints and Belle II sensitivity for visible and invisible axion-like particles, *J. High Energy Phys.* 12 (2017) 094, arXiv:1709.00009 [hep-ph].
- [35] W. Altmannshofer, et al., The Belle II physics book, *Prog. Theor. Exp. Phys.* 2019 (12) (2019) 123C01, arXiv:1808.10567 [hep-ex], 2019; Erratum: *Prog. Theor. Exp. Phys.* 2020 (2020) 029201.
- [36] Xabier Cid Vidal, Alberto Mariotti, Diego Redigolo, Filippo Sala, Kohsaku Tobioka, New axion searches at flavor factories, *J. High Energy Phys.* 01 (2019) 113, arXiv:1810.09452 [hep-ph]; Erratum: *J. High Energy Phys.* 06 (2020) 141.
- [37] Patrick deNiverville, Hye-Sung Lee, Min-Seok Seo, Implications of the dark axion portal for the muon g-2, B-factories, fixed target neutrino experiments and beam dumps, *Phys. Rev. D* 98 (11) (2018) 115011, arXiv:1806.00757 [hep-ph].
- [38] M.B. Gavela, R. Houtz, P. Quilez, R. Del Rey, O. Sumensari, Flavor constraints on electroweak ALP couplings, *Eur. Phys. J. C* 79 (5) (2019) 369, arXiv:1901.02031 [hep-ph].
- [39] L. Merlo, F. Pobbe, S. Rigolin, O. Sumensari, Revisiting the production of ALPs at B-factories, *J. High Energy Phys.* 06 (2019) 091, arXiv:1905.03259 [hep-ph].
- [40] Y.G. Aditya, Kristopher J. Healey, Alexey A. Petrov, Searching for super-WIMPs in leptonic heavy meson decays, *Phys. Lett. B* 710 (2012) 118–124, arXiv:1201.1007 [hep-ph].
- [41] G. Peter Lepage, Stanley J. Brodsky, Exclusive processes in perturbative quantum chromodynamics, *Phys. Rev. D* 22 (1980) 2157.
- [42] Adam Szczepaniak, Ernest M. Henley, Stanley J. Brodsky, Perturbative {QCD} effects in heavy meson decays, *Phys. Lett. B* 243 (1990) 287–292.
- [43] N. Satoyama, et al., A search for the rare leptonic decays $B^+ \rightarrow \mu^+ \nu(\mu)$ and $B^+ \rightarrow e^+ \nu(\nu)$, *Phys. Lett. B* 647 (2007) 67–73, arXiv:hep-ex/0611045.
- [44] M.T. Prim, et al., Search for $B^+ \rightarrow \mu^+ \nu_\mu$ and $B^+ \rightarrow \mu^+ N$ with inclusive tagging, *Phys. Rev. D* 101 (3) (2020) 032007, arXiv:1911.03186 [hep-ex].
- [45] I. Adachi, et al., Evidence for $B^- \rightarrow \tau^- \bar{\nu}_\tau$ with a hadronic tagging method using the full data sample of Belle, *Phys. Rev. Lett.* 110 (13) (2013) 131801, arXiv:1208.4678 [hep-ex].
- [46] B.I. Eisenstein, et al., Precision measurement of $B(D^+ \rightarrow \mu^+ \nu)$ and the pseudoscalar decay constant $f(D^+)$, *Phys. Rev. D* 78 (2008) 052003, arXiv:0806.2112 [hep-ex].
- [47] M. Ablikim, et al., Precision measurements of $B(D^+ \rightarrow \mu^+ \nu_\mu)$, the pseudoscalar decay constant f_{D^+} , and the quark mixing matrix element $|V_{cd}|$, *Phys. Rev. D* 89 (5) (2014) 051104, arXiv:1312.0374 [hep-ex].
- [48] Ablikim Medina, et al., Determination of the pseudoscalar decay constant $f_{D_s^+}$ via $D_s^+ \rightarrow \mu^+ \nu_\mu$, *Phys. Rev. Lett.* 122 (7) (2019) 071802, arXiv:1811.10890 [hep-ex].
- [49] Ablikim Medina, et al., Measurement of the $D_s^+ \rightarrow \ell^+ \nu_\ell$ branching fractions and the decay constant $f_{D_s^+}$, *Phys. Rev. D* 94 (7) (2016) 072004, arXiv:1608.06732 [hep-ex].
- [50] Ablikim Medina, et al., Observation of the leptonic decay $D^+ \rightarrow \tau^+ \nu_\tau$, *Phys. Rev. Lett.* 123 (21) (2019) 211802, arXiv:1908.08877 [hep-ex].
- [51] A. Zupanc, et al., Measurements of branching fractions of leptonic and hadronic D_s^+ meson decays and extraction of the D_s^+ meson decay constant, *J. High Energy Phys.* 09 (2013) 139, arXiv:1307.6240 [hep-ex].
- [52] C. Lazzeroni, et al., Precision measurement of the ratio of the charged kaon leptonic decay rates, *Phys. Lett. B* 719 (2013) 326–336, arXiv:1212.4012 [hep-ex].

- [53] F. Ambrosino, et al., Measurement of the charged kaon lifetime with the KLOE detector, *J. High Energy Phys.* 01 (2008) 073, arXiv:0712.1112 [hep-ex].
- [54] P.A. Zyla, et al., Review of particle physics, *PTEP* 2020 (8) (2020) 083C01.
- [55] Stanley J. Brodsky, G. Peter Lepage, Large angle two photon exclusive channels in quantum chromodynamics, *Phys. Rev. D* 24 (1981) 1808.
- [56] E. Armengaud, et al., Searches for electron interactions induced by new physics in the EDELWEISS-III Germanium bolometers, *Phys. Rev. D* 98 (8) (2018) 082004, arXiv:1808.02340 [hep-ex].
- [57] Asher Berlin, Nikita Blinov, Gordan Krnjaic, Philip Schuster, Natalia Toro, Dark matter, millicharges, axion and scalar particles, gauge bosons, and other new physics with LDMX, *Phys. Rev. D* 99 (7) (2019) 075001, arXiv:1807.01730 [hep-ph].
- [58] James B. Dent, Bhaskar Dutta, Doojin Kim, Shu Liao, Rupak Mahapatra, Kuver Sinha, Adrian Thompson, New directions for axion searches via scattering at reactor neutrino experiments, *Phys. Rev. Lett.* 124 (21) (2020) 211804, arXiv:1912.05733 [hep-ph].
- [59] Jean-François Fortin, Huai-Ke Guo, Steven P. Harris, Doojin Kim, Kuver Sinha, Chen Sun, Axions: from magnetars and neutron star mergers to beam dumps and BECs, *Int. J. Mod. Phys. D* 30 (07) (2021) 2130002, arXiv:2102.12503 [hep-ph].